Thermal Stress Analysis of Laminated Composite Solids of Axisymmetric Geometry

L. X. Sun* and T. R. Hsu†
University of Manitoba, Winnipeg, Manitoba, Canada

Introduction

LAMINATED composite materials have been used extensively in structures for commercial, military, and space applications. Abundant research has been carried out in the responses of this type of material to applied loads. Relatively little effort, however, was made in the assessment of thermal stresses induced by nonuniform temperature fields. Thermal distortion induced by some sources to structures made of laminated composite materials could be a major design consideration, e.g., in certain satellite components.[1] Thermomechanical behavior of laminated composite beams was investigated by Ochoa and Marcano.[2] Akoz and Tauchert[3] and Wang and Chou[4] presented solutions to both steady-state and transient thermal stresses in rectangular orthotropic slabs. Kalman and Tauchert attempted a solution for thermal stresses in orthotropic cylinders.[5] The stresses induced by uniform temperature in tubular structures were investigated by Hyer et al.[6] A recent study was conducted by Hyer and Cooper[7] on the thermal stress in tubes induced by circumferential temperature gradients. Almost all work reported in open literatures thus far are based on the classical theory of thermoelasticity. Versatility in solutions by the finite element method has not been fully realized in this type of analysis. For instance, no temperature variation across the thickness of tubes was allowed in the works by the above researchers. Further, variation of material properties due to change of temperature at high temperature environments was not included in the classical method.

This paper will present a formulation that allows the computation of temperature fields in axisymmetric structures made of laminated composite materials induced by heat fluxes from both radial and meridional directions. The discretization treatment of the structure by the finite element method allows the thermophysical properties of the materials to vary with local temperatures. The temperature field obtained from the thermal analysis is used to compute the associated thermal stresses in the structure. The formulation presented in this paper can be readily incorporated into existing programs developed for conventional engineering materials. Such implementation was carried out by using the TEPSAC code developed by the author T. R. Hsu for thermoelastic-plastic-creep stress analysis.[8] Numerical illustrations using the present analysis indicate strong influences of fiber orientations and stacking sequences on both the magnitude and distribution of resulting thermal stresses.

Finite Element Formulation on Thermal Analysis

The purpose of the analysis is to modify existing finite element formulation and algorithms suitable for laminate composite structures in an established TEPSAC code.[8] Following is a summary of key equations for the heat conduction analysis. Detailed derivation and descriptions of these equations can be found in Ref. 8.

Received March 27, 1989; revision received Aug. 23, 1989.

*Visiting Professor, currently at Nanjing Aeronautical Institute, Nanjing, China.

†Professor and Head, Department of Mechanical Engineering.

By referring to a typical triangular torus element with its nodal locations defined in an r-z coordinate system, the temperature in the nodes $\{T\}$ can be determined by

$$[K_e]\{T\} = \{f_e\} \tag{1}$$

in which $[K_e]$ is the thermal conductivity matrix and $\{f_e\}$ is the nodal thermal force matrix.

The thermal equilibrium equation for the entire structure, of course, can be assembled by following the usual procedure for the finite element analysis.

The element thermal conductivity matrix can be shown to take the form

$$[K_e] = \int_v [B(r,z)]^T[De][B(r,z)]\mathrm{d}v \tag{2}$$

in which the matrix $[B(r,z)]$ can be computed by differentiating the interpolation function $[N(r,z)]$ with respect to local coordinates as shown in Chap. 2 of Ref. 8.

For composite materials, the thermal conductivity coefficient matrix $[D_e]$ in the above formulation is defined by the principal material directions. These directions do not, in general, coincide with the global coordinates. A transformation is thus needed between the principal material directions and those defined by the global coordinates. The matrix $[D_e]$ in Eq. (1) can thus be expressed as

$$[D_e] = [T]^T[D_c][T] \tag{3}$$

in which the transformation matrix is

$$[T] = \begin{bmatrix} \cos\phi & -\sin\phi \\ \sin\phi & \cos\phi \end{bmatrix}$$

The angle ϕ is the angle between the principal material direction L and the r-axis direction (see Fig. 1) in the clockwise direction.

The thermal conductivity coefficient matrix defined by the local coordinates (principal material directions) has the form

$$[D_c] = \begin{bmatrix} k_1 & 0 \\ 0 & k_2 \end{bmatrix}$$

where k_1 and k_2 are the thermal conductivity coefficients in the respective principal material directions x_1 and x_2 (see Fig. 1).

The transformation matrices for each lamina in an element are the same and can be calculated according to the direction along the i-j side in the element as depicted in Fig. 1.

The reader is once again referred to Ref. 8 for the evaluation of the thermal force matrix $\{f_e\}$ in Eq. (1) and the formulation of the boundary conditions as well as computational algorithm.

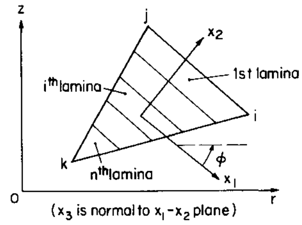

Fig. 1 Material and global coordinates for a torus element of laminated composite material.

Finite Element Formulation on Induced Thermal Stresses

For a discretized solid of axisymmetric geometry, the nodal displacements with two components each in a triangular torus element can be determined by similar element equations in Eq. (1).

The laminated composite material is assumed to obey the constitutive equation for orthotropic materials. Thus, for structures of axisymmetric geometry, the following relation applies:

$$\{\sigma\} = [C](\{\epsilon\} - \Delta T\{\alpha\}) \tag{4}$$

where $\{\alpha\}$ is the thermal expansion coefficient matrix of the material.

Elements of the $[C]$ matrix in Eq. (4) are available in Ref. 9. since material properties in the $[C]$ matrix along the principal directions may not coincide with the global coordinates (r,z); a proper adjustment is necessary by imposing a transformation matrix such that

$$[Ce] = [T]^T[C][T] \tag{5}$$

where the matrix $[Ce]$ may be considered to contain material properties that are consistent with the global coordinates.

The transformation matrix $[T]$ in Eq. (5) has been derived to take the form

$$[T] = \begin{bmatrix} \cos^2\phi & \sin^2\phi & 0 & 2\sin\phi\cos\phi \\ \sin^2\phi & \cos^2\phi & 0 & -2\sin\phi\cos\phi \\ 0 & 0 & 1 & 0 \\ -\sin\phi\cos\phi & \sin\phi\cos\phi & 0 & \cos^2\phi - \sin^2\phi \end{bmatrix}$$

Evaluation of the stiffness and nodal forces matrices by exact integration requires enormous time and effort. An approximate method is adopted in the present analysis. These matrices are evaluated by using average nodal coordinates as shown below

$$\bar{r} = (r_i + r_j + r_k)/3$$

and

$$\bar{z} = (z_i + z_j + z_k)/3$$

which leads to much simplified expressions for the stiffness and force matrices.

This averaging of coordinates in the computation also avoid the singular solutions at $r = 0$ for axisymmetric solids.

Numerical Illustration

The above formulation was implemented in an existing TEPSAC code.[8] A numerical example will be presented to demonstrate the capability of the finite element method.

The case under consideration involves a nose cone subjected to a steady-state heat influx from the outside surface. The cone has a parabolic profile defined by $z = -0.175r^2 + 70$ following the definition given in Fig. 2. There are 24 graphite-epoxy lamina in the cone. Each layer is 1.25 mm thick making the total thickness of 30 mm. Fibers are wound in either circumferential or meridional directions. Heat flux across the outside surface varies from q_1 to q_4 as illustrated in Fig. 2 with numerical values given as follows

$$q_1 = 0.3\ \text{W/mm}^2, \qquad q_2 = 0.01\ \text{W/mm}^2$$

$$q_3 = 0.001\ \text{W/mm}^2, \qquad q_4 = 0.0001\ \text{W/mm}^2$$

The inner surface of the core is kept at 0° C at all times.

The following material properties were used in the computations

1) Young's moduli, GPa: $E_1 = 147$; $E_2 = 9.1$; $E_3 = 9.93$
2) Shear moduli, GPa: $G_{12} = 4.27$; $G_{13} = 4.69$; $G_{23} = 5.93$
3) Poisson's ratios: $\nu_{12} = \nu_{13} = 0.3$; $\nu_{23} = 0.49$
4) Linear thermal expansion coefficients/C:

$$\alpha_1 = -7.7 \times 10^{-8};\ \alpha_2 = \alpha_3 = 33.7 \times 10^{-6}$$

5) Thermal conductivities, W/mm-C:

$$k_1 = 0.08;\ k_2 = k_3 = 0.008$$

The finite element mesh used for this case study involved 63 nodes and 48 elements. The temperature fields in the cone with various fiber orientations and stacking sequences resulting from the imposition of above thermal boundary conditions are depicted in Figs. 3 and 4. Figure 3 shows the temperature distributions in the cone with three pairs of stacking sequences; whereas Fig. 4 shows the induced temperature field in the nose cone with one pair of opposite stacking sequence of fibers. The following two observations on the numerical results can be made; 1) The top two sets of isothermal contours in Fig. 3 clearly indicate that temperature distribution is considerably more uniform in the case of fibers orienting along the axial direction. The other extreme, of course, is the case in which all fibers orient circumferentially. 2) For the equal number of plies and fiber orientations, the stackings which have fibers

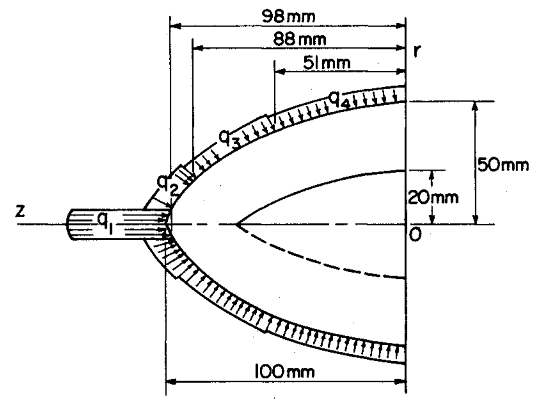

Fig. 2 Heat flux to a composite nose cone.

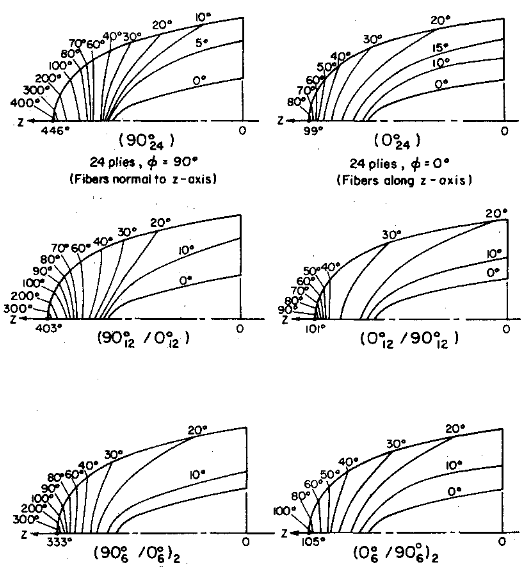

Fig. 3 Isothermal contours in a composite nose cone.

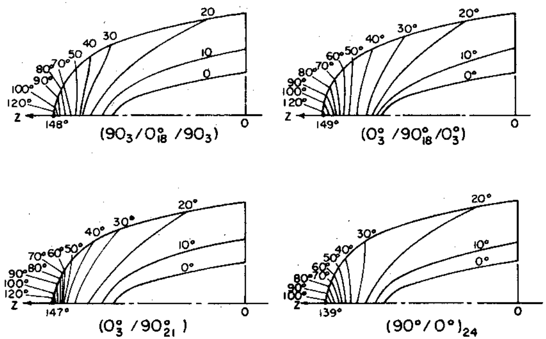

Fig. 4 Isothermal contours in a composite nose cone with various stacking sequences.

aligned axially near outer surfaces, e.g. (0 $\deg_{12}$/90 $\deg_{12}$) have lower peak temperature and temperature gradients than the cases otherwise. This is important as far as the induction of thermal stresses are concerned.

Thermal stresses associated with the induced thermal fields were also computed. Computed results indicated that the shear stresses are smaller than stresses along the fiber directions. It is not surprising to observe that modest thermal stresses exist in the cases in which more fibers are oriented along the meridional direction. A similar trend was observed for the thermal distortion of the cone.

Concluding Remarks

Numerical example has shown that both fiber orientation and stacking sequence play important roles in the distribution of temperature, thermal stresses, and distortion in the structure. The strong influence of stacking sequence on stress distribution is a well-known fact. However, this influence appears even more critical in the derivation of thermal stresses. This factor will thus become an important aspect in the design analysis of laminated composite structures subjected to thermal loads.

Acknowledgment

Authors wish to acknowledge the financial support of this research project provided by the Natural Science and Engineering Research Council of Canada.

References

[1]Hsu, T. R., and Lewak, R., "Measurements of Thermal Distortion of Laminated Fibre Composite Plates by Holographic Interferometry," *Experimental Mechanics*, May 1976, pp. 182–187.

[2]Ochoa, O. D., and Marcano, V. M., *Journal of Solid Structures*, Vol. 3, 1984, pp. 579–587.

[3]Akoz, A. Y., and Tauchert, T. R., *Journal of Mechanical Engineering Science*, Vol. 20, 1978, 00. 65–71.

[4]Wang, H. S., and Chou, T. W., *Journal of Composite Materials*, Vol. 19, 1985, pp. 424–442.

[5]Kalman, A. A., and Tauchert, T. R., *Journal of Thermal Stresses*, Vol. 1, 1978, pp. 13–24.

[6]Hyer, M. W., Cooper, D. E., and Cohen, D., *Journal of Thermal Stresses*, Vol. 9, 1986, pp. 97–117.

[7]Hyer, M. W., and Cooper, D. E., *Journal of Applied Mechanics*, Vol. 53, 1986, pp. 757–764.

[8]Hsu, T. R., *The Finite Element Method in Thermomechanics*. Allen & Unwin, Inc., Boston, 1986.

[9]Jones, R. M., *Mechanics of Composite Materials*. Scripta Book Co., Wash., DC, 1975.